Research Article

Received: 21 March 2022 Revised: 29 May 2022 Accepted article published: 8 June 2022 Published online in Wiley Online Library: 11 August 2022

(wileyonlinelibrary.com) DOI 10.1002/jctb.7153

Enhanced production of amylase, pyruvate and phenolic compounds from glucose by light-driven *Aspergillus niger*–CuS nanobiohybrids

Uddandarao Priyanka* and **Piet NL Lens**

Abstract

BACKGROUND: The demand for value-added compounds such as amylase, pyruvate and phenolic compounds produced by biological methods has prompted the rapid development of advanced technologies for their enhanced production. Nanobiohybrids (NBs) make use of both the microbial properties of whole-cell microorganisms and the light-harvesting efficiency of semiconductors. Photosynthetic NBs were constructed that link the biosynthetic pathways of *Aspergillus niger* with CuS nanoparticles.

RESULTS: In this work, NB formation was confirmed by negative values of the interaction energy, i.e., 2.31×10^8 to -5.52×10^8 kJ mol^{-1} for CuS–Che NBs, whereas for CuS–Bio NBs the values were -2.31×10^8 to -4.62×10^8 kJ mol^{-1} for CuS–Bio NBs with spherical nanoparticle interaction. For CuS–Bio NBs with nanorod interaction, it ranged from -2.3×10^7 to -3.47×10^7 kJ mol^{-1}. Further, the morphological changes observed by scanning electron microscopy showed the presence of the elements Cu and S in the energy-dispersive X-ray spectra and the presence of CuS bonds in Fourier transform infrared spectroscopy indicate NB formation. In addition, the quenching effect in photoluminescence studies confirmed NB formation. Production yields of amylase, phenolic compounds and pyruvate amounted to 11.2 μmol L^{-1}, 52.5 μmol L^{-1} and 28 nmol μL^{-1}, respectively, in *A. niger*–CuS Bio NBs on the third day of incubation in the bioreactor. Moreover, *A niger* cells–CuS Bio NBs had amino acids and lipid yields of 6.2 mg mL^{-1} and 26.5 mg L^{-1}, respectively. Furthermore, probable mechanisms for the enhanced production of amylase, pyruvate and phenolic compounds are proposed.

CONCLUSION: *Aspergillus niger*–CuS NBs were used for the production of the amylase enzyme and value-added compounds such as pyruvate and phenolic compounds. *Aspergillus niger*–CuS Bio NBs showed a greater efficiency compared to *A. niger*–CuS Che NBs as the biologically produced CuS nanoparticles had a higher compatibility with *A. niger* cells.

Supporting information may be found in the online version of this article.

Keywords: α-amylase; *Aspergillus niger*; CuS nanoparticles; nanobiohybrid; phenol; pyruvate

INTRODUCTION

With an increase in population globally, use of industrial enzymes has been extended in recent years to a variety of fields such as food production, brewing, pharmacy, medicine, textile and detergents.[1] Generally, natural products are considered attractive value-added compounds based on their wide bioactivity spectrum[2]. α-Amylases are extracellular enzymes that cleave the α-1,4-glucosidic bonding of linear amylose and branching amylopectin. They are the most important group of enzymes produced commercially[3]. α-Amylase, belonging to the glycosyl hydrolase family, is a digestive enzyme that catalyses the hydrolysis of starch, glycogen and related polysaccharides and, therefore, has wide applications in many industries. α-Amylases have not only been used in fermentation processes but also in the processed food industry and the textile and paper industries[3]. Compared with the bacterial α-amylases, fungal α-amylases are preferred for starch hydrolysis applications in the baking, brewing and sweeteners industries owing to their generally recognized safe status.[4]

Pyruvate has many important applications, e.g. as a food supplement and as a precursor for chemicals and pharmaceuticals. This compound has both reactive ketonic and carboxyl groups

* *Correspondence to: U Priyanka, Department of Microbiology and Ryan Institute, National University of Ireland, University Road, Galway, Ireland. E-mail: priyanka.uddandarao@nuigalway.ie*

Department of Microbiology and Ryan Institute, National University of Ireland, Galway, Ireland

and its demand has greatly increased over the past few decades.[5] It is also manufactured for use as a dietary supplement, nutraceutical and antioxidant. For example, pyruvate is used as a promising raw material for the synthesis of pharmaceutical precursors such as L-tyrosine, *N*-acetyl-D-neuraminic acid and (*R*)-phenylacetylcarbinol.[6] Phenolic compounds are widespread phytochemicals in nature; usually plant extracts rich in phenolic compounds have shown increasingly interest to enhance food quality. Therapeutic use as functional ingredients is the basis of numerous studies on how processing affects the phenolic composition of foods and the bioactivity of nanoencapsulated phenolics on cancer cells.[7] Phenolic compounds consist of an aromatic ring bearing one or more hydroxyl substituents, and range from simple phenolic molecules to highly polymerized compounds.[8]

In spite of these advantages, the use of enzymes and food additives in industrial applications suffers from cost limitations.[9] From a bio-industrial viewpoint, microorganisms are the most important sources for the production of value-added chemicals.[10] Filamentous fungi have the ability to synthesize and secrete large amounts of extracellular protein, making filamentous fungi attractive hosts for production of value-added products.[11] CuS as an important multifunctional I–VI chalcogenide visible-light-absorbing semiconductor[12] and has received widespread attention because of its versatile properties, and has great potential in a versatile range of applications such as cathode material of lithium batteries, gas sensors, photocatalysts, photothermal conversion and high-temperature thermistors.[13–15] In this scenario, nanobiohybrids (NBs) came into the picture, where microbes possess more desirable metabolic pathways when integrated with nanoparticles (NPs), offering tunable microbial metabolism.[16,17] In this study, we demonstrate a hybrid approach, by integrating *Aspergillus niger* with photoactive CuS NPs to synthesize amylase, pyruvate and phenolic compounds from a medium consisting of glucose (8 g L^{-1}) and ammonium sulfate (3 g L^{-1}).

The first step towards the development of NBs is assembly, for chemically/biologically and energetically coupling the NPs with *A. niger* cells. The NBs were designed by choosing an NP active in the visible-light region. The key objectives of the present study are: (i) to synthesize chemical and biological CuS NPs by the precipitation method and sulfate reduction method, respectively; (ii) to bind the synthesized CuS NPs with *A. niger* cells to form NBs; and (iii) to produce metabolites such as amylase, pyruvate and phenolic compounds using the CuS–*A. niger* NBs.

MATERIALS AND METHODS

Aspergillus niger cultivation

Aspergillus niger *strain*

The *A. niger* strain was isolated from effluent of an anaerobic inverse fluidized bed bioreactor treating selenite-rich wastewater.[18] The *A. niger* strain was grown on Petri plates with potato dextrose agar (PDA) medium and incubated at 28 °C. The spores were collected from the Petri plates using a loop and stored at −20 °C until future use in the experiments.[19]

Batch cultivation

For the preliminary experiments, shake flask cultivation was conducted in 250 mL Erlenmeyer flasks with a 100 mL working volume of potato dextrose broth medium to which 2×10^5 mL^{-1} *A. niger* spores were added. The inoculated flasks were incubated on a rotary shaker at 1157 g and 30 °C. After 2 days of growth, once the *A. niger* cells attained the log phase, they were used for NB formation by adding chemically and biologically synthesized CuS NPs.[20,21]

CuS NP synthesis

Chemical synthesis route

For the chemical synthesis of CuS NPs, 50 mL of 1 mol L^{-1} copper acetate monohydrate ($Cu(CH_3COO)_2.H_2O$) and 1 mol L^{-1} sodium sulfide ($Na_2S.9H_2O$) precursors were added to 250 mL Erlenmeyer flasks; 2 mol L^{-1} NaOH was further added to the precursor solution until it reached pH 11 at room temperature.[90] The precursors undergo a decomposition reaction and the addition of NaOH to the reactants induces a precipitation reaction leading to the formation of a blue-green precipitate after 2 h (Eqn (1)):[15,22]

$$Cu(CH_3COO)_2.H_2O + Na_2S.9H_2O \rightarrow CuS + 2CH_3COONa + 10H_2O \quad (1)$$

The precipitate was dried at 80 °C in a hot-air oven for 4–5 h and stored at 28 °C for further use.[23]

Biological synthesis route

Biological CuS NPs were synthesized using anaerobic granular sludge collected from an upflow anaerobic sludge blanket reactor (Kilconnell, Galway, Ireland) containing sulfate-reducing bacteria.[24] The inoculum had a total solids (TS) content of 62.5 g kg^{-1} wet granular sludge and its volatile solids (VS)/TS ratio was 89%, yielding a VS concentration of 55.6 g kg^{-1} wet granular sludge.[25] It was incubated in a medium of 3 g $(NH_4)_2SO_4$, 0.126 g K_2HPO_4, 0.875 g $MgSO_4.7H_2O$ and 1.5 g $Ca(NO_3)_2.4H_2O$. 50 mL of 60% (v/v) glucose was taken as the carbon source. The pH of the medium was adjusted to 7 using 1 mol L^{-1} NaOH. 10% (v/v) of the anaerobic sludge was added to a 500 mL serum bottle containing 300 mL medium and the bottles were purged with nitrogen gas before and after inoculation.

The serum bottles were incubated in an orbital shaker set at 30 °C and 1035 g for 7 days. After the reduction of sulfate to sulfide, 50 mL supernatant from 300 mL anaerobic sludge was added to 50 mL of 1 mol L^{-1} copper(II) sulfate pentahydrate solution ($CuSO_4.5H_2O$) while stirring for 7 days. The sulfide produced by the anaerobic sludge reacted with the copper(II) and precipitated as CuS to form biologically synthesized CuS NPs (CuS-Bio NPs) (Eqn (2)):[26,27]

$$CuSO_4.5H_2O + S \rightarrow CuS + 5H_2O + SO_2 + O_2 \quad (2)$$

Aspergillus niger *cells–CuS NBs*

The approach adopted for fabrication of *A. niger* CuS NP NBs was carried out based on the Derjaguin–Landau–Verwey–Overbeek (DLVO) theory of Derjaguin approximation,[28,29] which describes the interaction between *A. niger* cells and CuS NPs as a sum of van der Waals attractive and electrostatic repulsive force. *Aspergillus niger* cells were added to CuS NPs present in the potato dextrose broth medium, to which 1 mmol L^{-1} sodium chloride (NaCl) was added dropwise at regular time intervals[30,31] and stirred for 4 h. The amount of biomass used was 32.5 g L^{-1}. A colour change was observed after 4 h, indicating the formation of NBs. The binding of *A. niger* cells and CuS NPs is confirmed by values of $W(D)$ of -2.31×10^8 to -5.52×10^8 kJ mol^{-1} for CuS–Che NBs, as well as for CuS–Bio NBs $W(D)$ values from -2.31×10^8 to -4.62×10^8 kJ mol^{-1} for spherical NPs and from -2.3×10^7 to -3.47×10^7 kJ mol^{-1} for nanorods. The net interaction energy

Journal of Chemical Technology and Biotechnology published by John Wiley & Sons Ltd on behalf of Society of Chemical Industry (SCI).

between *A. niger* cells and CuS NPs was calculated as described by Uddandarao and Lens.[32,33]

Experimental set-up

A cylindrical bench-scale stirred tank photobioreactor made of Pyrex glass (2.5 L capacity and 1.5 L working volume) was used for the experiments. The medium composition consisted of 8.0 g L^{-1} glucose and 3.0 g L^{-1} ammonium sulfate.[34] During the reaction phase, the *A. niger* NBs were mixed with a magnetic stirrer for aeration at 1035 g. The temperature was maintained at 30 °C. A visible-light source of wavelength 400 nm (11935–55 LED lamp, Leuchten Direkt, Galway, Ireland) was placed at 2 cm distance from the stirred tank photobioreactor. The photobioreactor was operated with a hydraulic retention time (HRT) of 5 days (Fig. 1). Samples were withdrawn intermittently from the top of the sampling port for analysis. The experiments were conducted in five sets: (a) *A. niger* cells; (b) *A. niger* cells with CuS–Che NPs; (c) *A. niger* cells with CuS–Bio NPs; (d) CuS–Che NBs; and (e) CuS–Bio NBs. Sets (a), (b) and (c) were considered as control experiments.

Product recovery and quantification

For the recovery of pyruvate, cell disruption was carried out by ultrasonication for 30 min with 10 min intervals three times.[35] *Aspergillus niger* cell pellets were suspended in lysis buffer (50 mmol L^{-1} Tris–HCl (pH 8.0, 0.1% (v/v) Triton). The cell lysate from the cell disruption treatment was clarified by centrifugation at 5488 × *g* for 10 min. This sample was used for total sugars and pyruvate quantification. For recovery of amylase and phenolic compounds, liquid–liquid extraction was carried out, for which the extracellular components were purified by 25% ammonium sulfate precipitation.[36,37]

Total sugars

Quantification of the total sugar concentration was carried out by the sulfuric acid method.[38] A 1 mL aliquot of sample solution was rapidly mixed with 3 mL concentrated sulfuric acid in a test tube and vortexed for 30 s. The temperature of the mixture rises rapidly within 10–15 s after sulfuric acid addition; the solution was therefore cooled on ice for 2 min to bring it to room temperature. Absorption at 315 nm was read using a UV–visible spectrophotometer. Standard solutions were prepared similarly to the sample preparation procedure.[39]

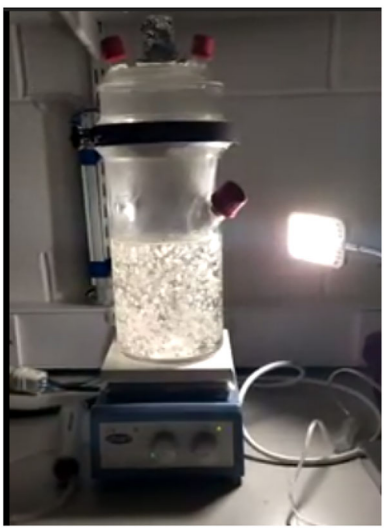

Figure 1. Photograph of stirred tank photobioreactor containing CuS–Bio NBs.

Assays of amylase activity

Amylase activity was determined using soluble starch (1%, w/v) as the substrate, dissolved in 0.05 mol L^{-1} sodium phosphate buffer (pH 6.5). The final reaction mixture, prepared by adding 1.8 mL starch solution (1 g L^{-1}) and 0.2 mL enzyme solution (0.05 g L^{-1}), was incubated at 50 °C for 10 min. The reaction was stopped by adding 3 mL dinitrosalicylic acid (DNS) as described by Miller.[40] The amylase was determined by taking absorbance at 540 nm with a UV–visible spectrophotometer (Shimadzu UV-1800, Duisburg, Germany). One unit of amylase activity denotes the amount of enzyme required for releasing 1 g L^{-1} reducing sugar per minute under assay conditions.[20,41–43]

Pyruvate determination

Pyruvate concentration was measured following the protocol given in the pyruvate assay kit (MAK071-1KT, Sigma-Aldrich, Saint Louis, USA). As with the colorimetric assay, 1 nmol mL^{-1} standard solution was prepared. Further, to generate 0.1 nmol mL^{-1} standard solution, 10 mL of the 1 nmol mL^{-1} standard solution was diluted with 90 mL of the pyruvate assay buffer. 0, 2, 4, 6, 8 and 10 mL solutions were added to each well (0.1 nmol mL^{-1} standard solution), resulting in 0, 0.2, 0.4, 0.6, 0.8 and 1.0 nmol standards, and 50 mL pyruvate assay buffer. Samples were prepared similarly to standards.

Lipid yield

Aspergillus niger biomass was harvested by filtration, washed twice with distilled water and centrifuged at 5488 × *g* for 15 min. Dry biomass was determined based on constant weight at 105 °C. The *A. niger* biomass was used for lipid extraction. The lipid was extracted by the method of Folch *et al.*[93]

Total amino acids

The protein content of the enzyme extract was estimated by the Lowry method[44] using bovine serum albumin (BSA) as the standard.[45] The calibration curve was plotted using standard protein BSA.

Total phenols

The total phenolic content was determined colorimetrically using the Folin–Ciocalteu (FC) method. Test samples (0.5 mL) were mixed with 0.2 mL FC reagent and allowed to stand for 10 min; 0.6 mL of 20% sodium carbonate was added and mixed completely. The reaction mixture was incubated at 40 °C for 30 min. Absorbance of the reaction mixture was measured at 765 nm. Gallic acid was taken as standard.[46–48]

Characterization techniques

Transmission electron microscopy (TEM) was performed as described by Uddandarao and Lens.[32,33] Oven-dried CuS–Che NPs and lyophilized CuS–Bio NPs were dispersed in ethanol. A drop of this was placed on the copper grids using a pipette and kept overnight under vacuum in a desiccator. From these grids, images were collected on a Hitachi H-7000 transmission electron microscope (Uedem, Germany). CuS–Che NBs and CuS–Bio NBs were placed on a cover slip and kept overnight in a vacuum desiccator. Later, the samples were sputtered with gold and loaded onto a specimen holder for analysis by scanning electron

microscopy (SEM) coupled to energy-dispersive X-ray spectroscopy (EDX; Hitachi S2600N variable pressure scanning electron microscope)[49,50].

Analytical methods

X-ray diffraction (XRD) patterns were measured between percentage intensities of 20° and 60° (2θ) using Cu-Kα radiation at a wavelength of 1.54 Å operating at 35 kV and 25 mA (Inel Equinox 6000 powder, Waltham, Massachusetts, USA). Crystallite size was calculated by employing the Debye Scherrer equation in Supporting Information (Eqn (S7)).

Optical absorption spectra of the samples were recorded from 200 to 900 nm using a UV–visible spectrophotometer (Shimadzu UV-1800). Tauc plots were used to estimate the band gap (E_g) of both CuS–Che NPs and CuS–Bio NPs[51] based on the UV–visible spectra (Supporting Information, Eqns (S3), (S4)). The number of photons arriving per second was calculated from Eqn (S2). The band edge positions of the valence band (E_{VB}) and the conduction band (E_{CB}) edge potentials of the CuS NPs were determined from Eqns (S5) and (S6). A Fourier transform infrared (FTIR) spectrometer in the spectral range of 4000–600 cm^{-1} with a 4 cm^{-1} resolution was operated at attenuated total reflection (ATR) mode (Nicolet iS5, Thermo Scientific, Waltham, MA, USA).[52]

The total organic carbon measurements were assessed using a total organic carbon analyser (TOC-L, Shimadzu, Hamburg, Germany). Photoluminescence spectra were achieved through fluorescence measurements (Fluorolog 3 TCSPC, Horiba, Japan) using a xenon lamp as an excitation source and grating of 1200 g mm^{-1}. All measurements were performed at room temperature.

RESULTS

CuS NP synthesis

The chemical precipitation method produced a blue-green precipitate, consisting of spherical CuS NPs with an average size range of 10–24 nm (Fig. 2a). The sulfate reduction method produced a dark-brown precipitate, consisting of both spherical NPs and nanorods of an average size range of 10–20 nm and 100–150 nm, respectively (Fig. 2b). UV–visible spectra exhibited strong absorption in the entire visible region (Supporting Information, Fig. S1a,c). This intense absorption in the entire visible range implies that CuS NPs are good visible-light harvesters.[53] The absorption edge of these CuS–Che NPs and CuS–Bio NPs is positioned at, respectively, 953.85 nm and 775 nm according to the band gap values (E_{bg}) of 1.3 eV (Fig. S1b) and 1.6 eV (Fig. S1d).

The efficiency of a semiconductor photocatalyst relies primarily on the electron generation ability of the material at the surface, which is governed by the energetics of the conduction and valence bands. The absolute positions of the E_{CB} and E_{VB} band edges were calculated for Che–CuS NPs to be 0.58 and − 0.72 eV, respectively; and 0.73 and − 0.87 eV, respectively for Bio–CuS NPs. The valance band values are thus higher for Bio–CuS NPs than for Che–CuS NPs, indicating a higher electron production.[54–57] Photon energy (E_{ph}) corresponding to a wavelength of 953.85 nm produced 1.04×10^{11} photons s^{-1} for CuS–Che NPs, whereas a wavelength of 775 nm produced 1.29×10^{11} photons s^{-1} for CuS–Bio NPs. Further, diffraction at 2θ values showed peaks at (100), (102), (110), (108) and (116) (Fig. 3a) that are perfectly indexed to the hexagonal phase of CuS and is comparable with the ICCD card No. 06–0464.[15] The average crystallite size of the CuS–Che NPs is 1.21 nm. The diffraction peaks corresponded to (002), (111), (202), (020), (113), (311) and (220) for CuS–Bio NPs (Fig. 3b), which is on a par with ICCD card No. 78–0876.[22] The average crystallite size of the CuS–Bio NPs is 1.07 nm.

Aspergillus niger cells–CuS NB formation

Dense growth and thickening of the hyphae were observed in SEM images of CuS–Che NBs (Fig. 4b) and CuS–Bio NBs (Fig. 4c), indicating the presence of CuS NPs. Such modification on the *A. niger* cell surface indicated the production of intracellular compounds, and cell wall protrusions increased the formation of intracellular vacuoles, resulting in bulging of mycelia, leading to the outward growth of cell wall structures.[58,59] *Aspergillus niger* cells without the addition of CuS NPs are the control (Fig. 4a). Further, the binding of *A. niger* cells and CuS NPs is confirmed by $W(D)$ values of -2.31×10^8 to -5.52×10^8 kJ mol^{-1} for CuS–Che NBs, as well as for CuS–Bio NBs $W(D)$ values from -2.31×10^8 to -4.62×10^8 kJ mol^{-1} for spherical NPs and from -2.3×10^7 to -3.47×10^7 kJ mol^{-1} for nanorods. Subsequently, for CuS–Che NBs, the EDX data (Fig. 3d) showed copper (Cu) and sulfide (S) peaks. The oxygen (O), carbon (C) and aluminium (Al) peaks correspond to the medium components, the gold (Au) peak is due to sputtering and the sodium (Na) peak is due to impurities present in the CuS–Che NPs. Besides, the EDX pattern (Fig. 3e) of CuS–Bio NBs affirms the presence of copper (Cu) and sulfide (S). The carbon (C), oxygen (O), sodium (Na), iron (Fe) and aluminium (Al) peaks are due to the medium components and the gold (Au) peak to sputter coating of the sample during TEM sample preparation.

The presence of vibrational peaks at 618 and 872 cm^{-1} in the FTIR spectra of the CuS–Che NPs indicates the Cu—S stretching modes,[49] the 1136 cm^{-1} peak corresponds to C—N stretching and the 1425 cm^{-1} peak corresponds to C—C stretching, as shown in Fig. 5(a). In CuS–Che NBs, 637 and 872 cm^{-1} peaks appeared in the FTIR spectra, indicating the presence of CuS–Che NPs. The peak at 1014 cm^{-1} corresponds to stretching vibrations of C═O groups of amides (amide I) or stretching vibrations of C—N; the peak at 1425 cm^{-1} confirms the presence of COO$^-$ groups in the sample; the 1720 cm^{-1} peak is the ester C═O stretch of lipid triglycerides; and the 3128 cm^{-1} peak corresponds to the bending modes of H—O—H moieties of absorbed water by CuS NPs (Fig. 5d). Similarly, in CuS–Bio NPs, the peaks at 610 and 838 cm^{-1} indicate Cu—S stretching modes; the 1109 cm^{-1} peak is the C—N stretch and the 1402 cm^{-1} peak is the C—C stretch; the 1564 cm^{-1} peak is the amide II (protein in N—H bend, C—N stretch) and the 3305 cm^{-1} peak is the O—H stretch (Fig. 5b). The presence of vibrational peaks around 637 and 872 cm^{-1} are due to the presence of Cu—S stretching modes indicating the presence of CuS–Bio NPs. The 1109 cm^{-1} peak is the C—N stretch and the peak 1398 cm^{-1} is the C—C stretch; the 1720 cm^{-1} peak is the ester C═O stretch of lipid triglycerides; and the 3128 cm^{-1} peak corresponds to the bending modes of H—O—H moieties of absorbed water by CuS Bio NBs (Fig. 5e). Control experiments of *A. niger* cells show peaks at 1014, 1398 and 1647 cm^{-1}, representing vibrations for C═C, and the peak at 3128 cm^{-1} corresponds to water molecules (Fig. 5c).[60–63]

Figure 6(a) plots an overlay of the photoluminescence emission spectra at 530 nm, and shows a narrow peak corresponding to intensity 5.7×10^5 (a.u.) for CuS–Che NPs and 1.52×10^6 (a.u.) CuS–Bio NPs, respectively, while the bare *A. niger* solution shows no photoluminescence emission. However, CuS–Bio NPs showed more quenching effects than CuS–Che NPs. Before carrying out the light exposure experiments, the photoluminescence emission

Journal of Chemical Technology and Biotechnology published by John Wiley & Sons Ltd on behalf of Society of Chemical Industry (SCI).

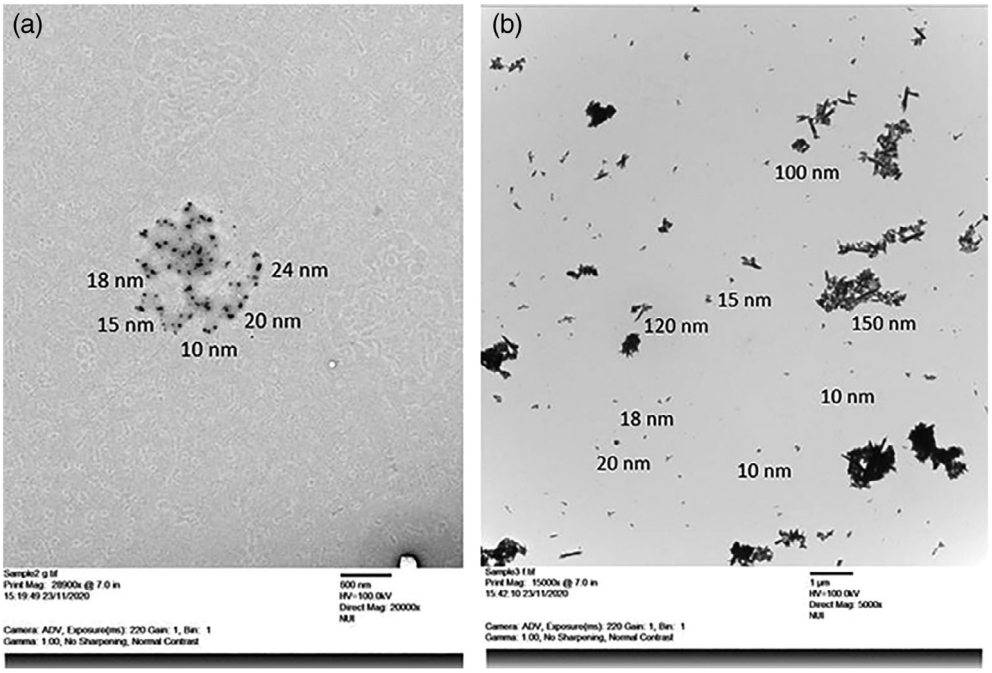

Figure 2. TEM image of (a) CuS–Che and (b) CuS–Bio NPs.

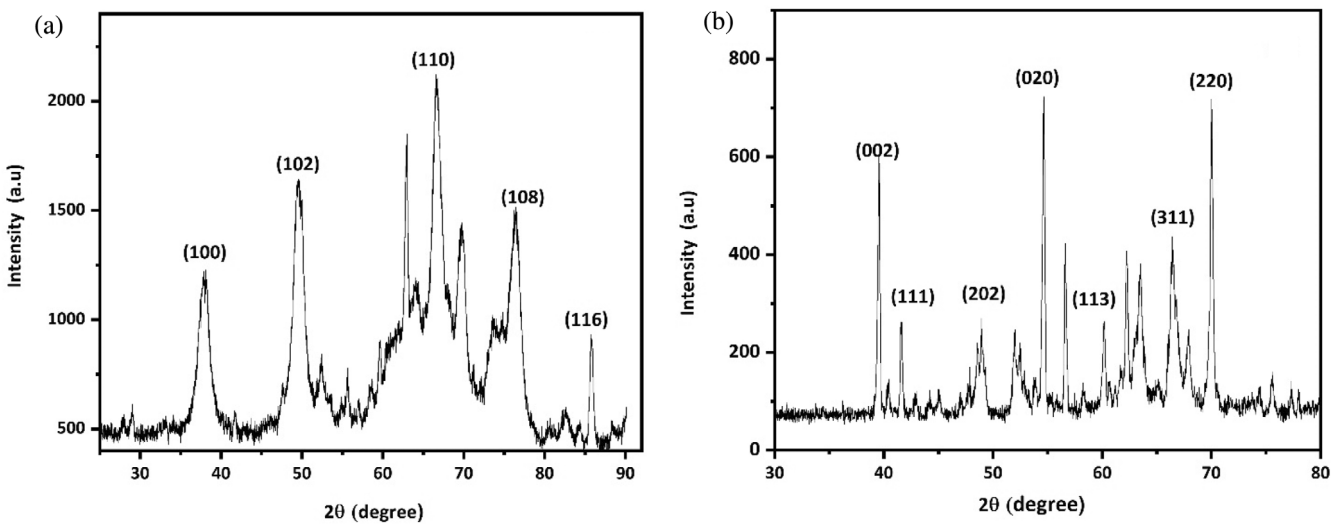

Figure 3. XRD pattern of (a) CuS–Che and (b) CuS–Bio NPs.

spectrum of the *A. niger*–CuS system gives a broader peak with visible light than the bare CuS NPs solution. However, during the light exposure experiments, the photoluminescence emission of the *A. niger*–CuS–Che NBs and *A. niger*–CuS–Bio NBs solution is totally quenched compared to *A. niger*–CuS–Che NPs and *A. niger*–CuS–Bio NPs (Fig. 6b). Thus it can be concluded that, instead of undergoing a recombination process, photoexcited electrons from the CuS NPs are transferred to the cytoplasm and distributed among the redox mediators of the *A. niger* cells.

Production on amylase, pyruvate, phenols and TOC

The incubation was started as a normal batch mode for the first 48 h. The *A. niger* cells from the shake flask were transferred to the stirred tank 2.5 L photobioreactor. When the *A. niger* cells attained the late log phase after 96 h incubation, the maximum amylase activity was observed on the third day after transferring to the reactor, i.e. 6, 6.4, 6.8, 10.16 and 11.2 μmol mL^{-1} for *A. niger* cells, *A. niger* cells–CuS–Che NPs, *A. niger* cells–CuS–Bio NPs, *A. niger* cells–CuS–Che NBs and *A. niger* cells–CuS–Bio NBs, respectively, in the presence of visible light by utilizing approximately 3 g L^{-1} glucose (Fig. 7a,b). However, amylase activity in the absence of light amounted to 4 μmol mL^{-1} for *A. niger* cells utilizing 2.2 g L^{-1} glucose (Fig. 7a,b). After the third day in the reactor, it reached the stationary phase and the amylase activity gradually declined.

The *A. niger* cells possessed a high total phenol content yielding 10.6 μmol mL^{-1} in the absence of light. The phenols amounted to 16.4, 26.2, 26.5, 50.2 and 52.5 μmol mL^{-1} for *A. niger* cells, *A. niger*

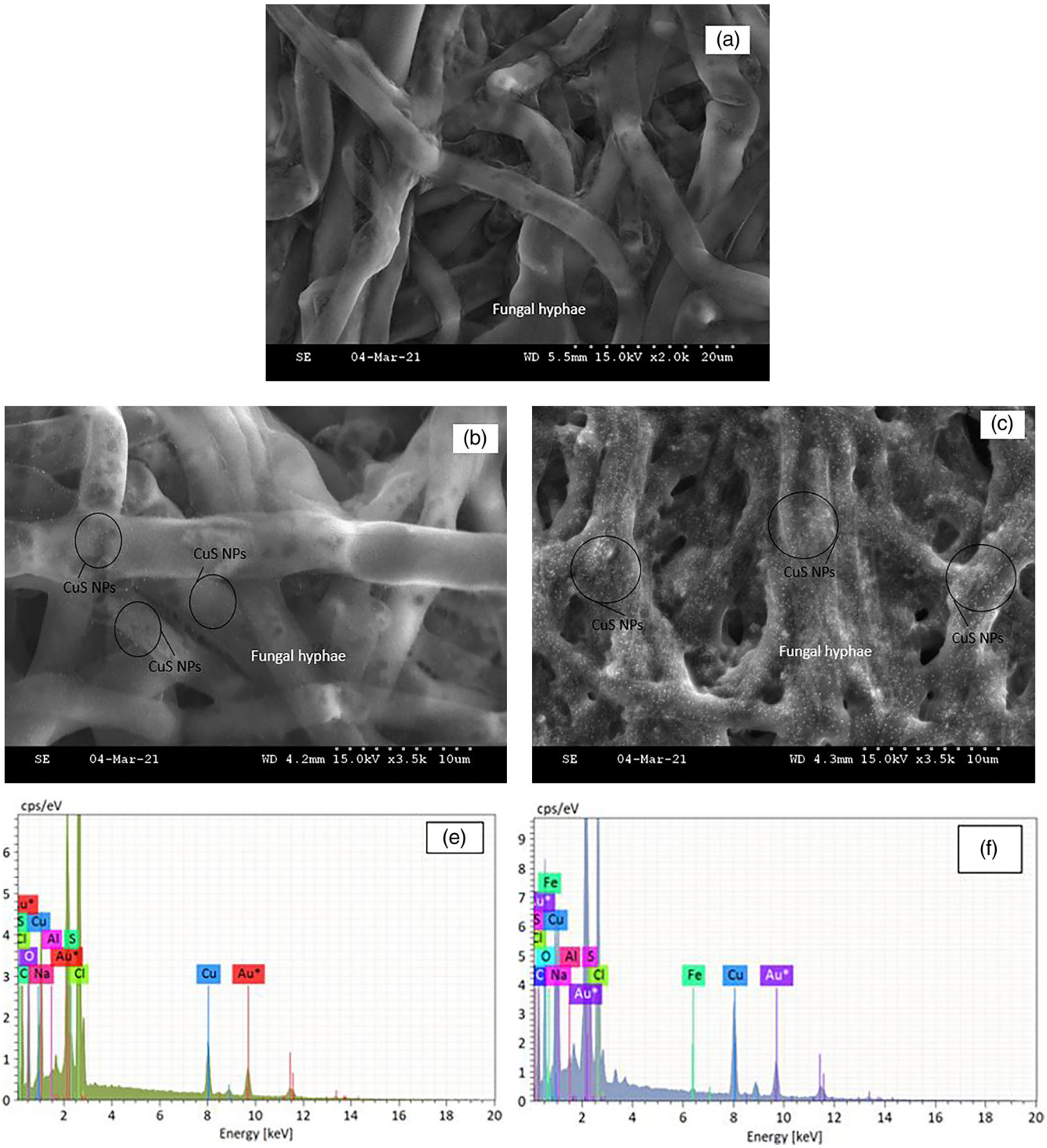

Figure 4. SEM images of the (a) *A. niger* cells, (b) CuS–Che and (c) CuS–Bio NBs, as well as EDX images of (d) CuS–Che and (e) CuS–Bio NBs.

cells–CuS–Che NPs, *A. niger* cells–CuS–Bio NPs, *A. niger* cells–CuS–Che NBs and *A. niger* cells–CuS–Bio NBs, respectively, in the presence of light (Fig. 7c). In the same period, the pyruvate concentration was 9 nmol μL^{-1} *A. niger* cells in the absence of light. The pyruvate yield amounted to 18.95, 25, 25.5, 27.5 and 28 nmol μL^{-1} for *A. niger* cells, *A. niger* cells–CuS–Che NPs, *A niger* cells–CuS–Bio NPs, *A. niger* cells–CuS–Che NBs, *A. niger cells*–CuS–Bio NBs, respectively, in the presence of visible light (Fig. 7d). Along with the increase in efficiency in the presence of light, the amount of TOC generated also increased around 2.7, 2.8 and 2.9 times for *A. niger* cells, *A. niger* cells–CuS–Che NPs and *A. niger* cells–CuS–Bio NPs, respectively, and a 3.1 times increase for *A. niger* cells–CuS–Che NBs and *A. niger* cells–CuS–Bio NBs in comparison to dark conditions (Fig. 7e). Quantum efficiency is defined by the ratio of the effective electrons used for amylase, pyruvate and total phenol production to the total input photon flux

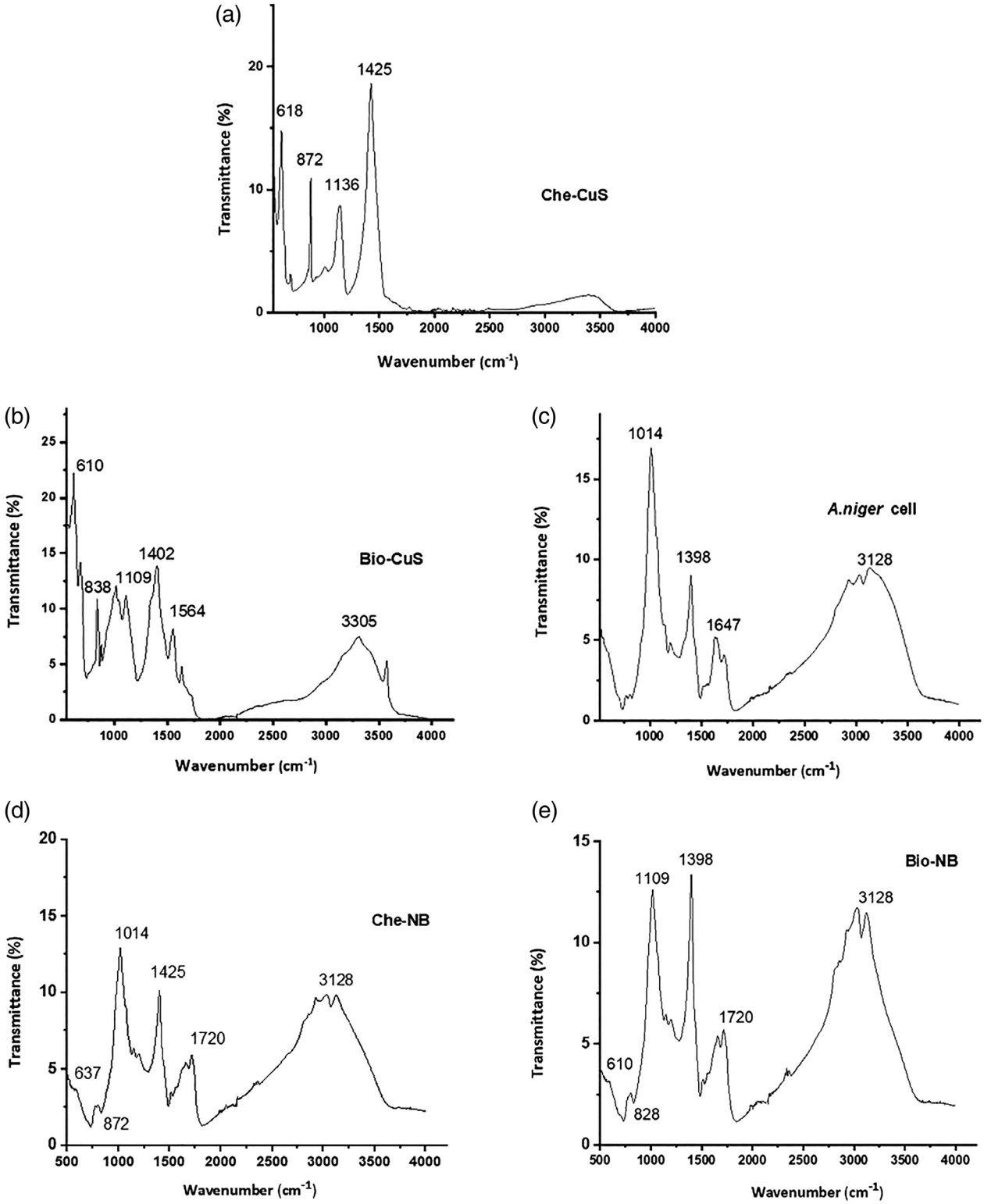

Figure 5. FTIR spectra of (a) *A. niger* cells, (b) CuS–Che and (c) CuS–Bio NPs, as well as (d) CuS–Che and (e) CuS–Bio NBs.

(Supporting Information, Table S1). The amylase, pyruvate and total phenolic compound content was higher in *A. niger* cells–CuS–Bio NBs compared to *A. niger* cells–CuS–Che NBs as the biologically synthesized NPs have higher compatibility to *A. niger* cells than CuS Che NPs.

Amino acid content and lipid yield in NBs

The total amino acid content in the *A. niger* cells–CuS NBs remained the same with the amylase, phenolic compound and pyruvate production (Fig. 8a). This is because the membrane proteins play a role in the electron transport chain; therefore NPs did

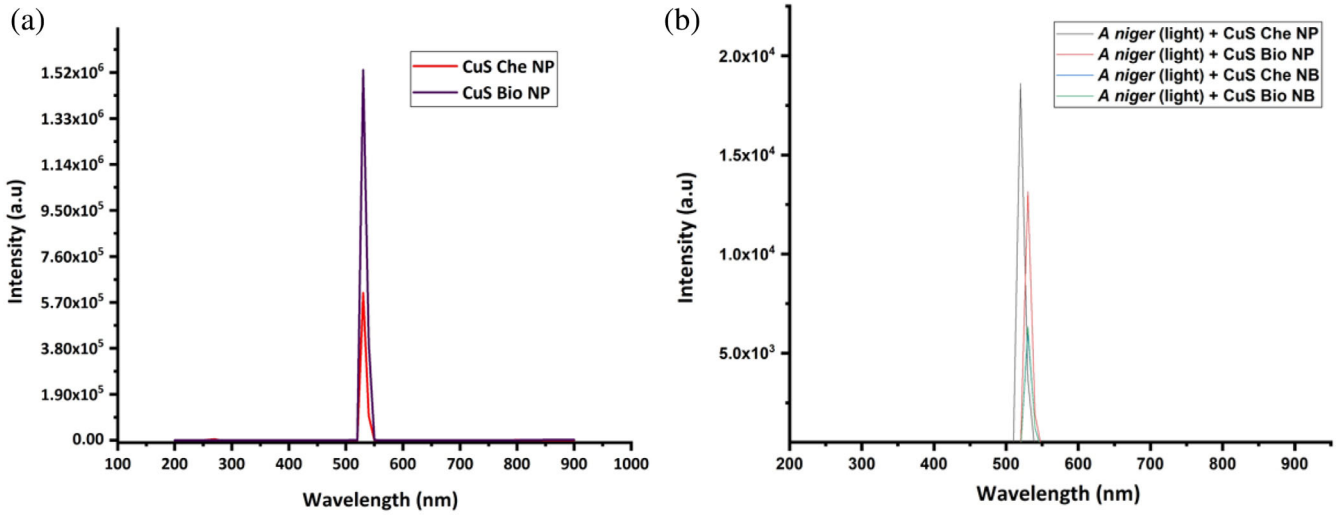

Figure 6. Photoluminescence spectra of (a) CuS–Che and CuS–Bio NPs, as well as (b) *A. niger* cells with CuS–Che NPs and CuS–Bio NPs (added separately), *A. niger*–CuS–Che and *A. niger*–CuS–Bio NBs.

not influence the amino acid yield.[64,65] The total amino acid content amounted to 5.8 mg mL^{-1} for *A. niger* cell dry weight, 6 mg mL^{-1} for *A. niger*–CuS–Che NPs, and 6.2 mg mL^{-1} for *A. niger*–CuS–Bio NPs, *A. niger*–CuS–Che NBs and *A. niger*–CuS–Bio NBs, respectively (Fig. 8a).

Aspergillus niger has the ability to produce substantial amounts of storage lipids.[66,67] The biomass dry weight slightly decreased in the presence of light and upon the addition of CuS NPs, corresponding to a biomass weight of 20.2 g L^{-1} for *A. niger* cells in the dark, 24.5 g L^{-1} for *A. niger* cells in the presence of light, and 25.7 g L^{-1} for *A. niger*–CuS–Che NPs, 25.8 g L^{-1} for *A. niger*–CuS–Bio NPs, 26.4 g L^{-1} for *A. niger*–CuS–Che NBs and 26.5 g L^{-1} for *A. niger*–CuS–Bio NBs (Fig. 8b). On the other hand, under these conditions, it was found that the *A. niger* biomass (Fig. 8b) continued to increase for 5 days. Lipid yields were correlated with the generated biomass, as shown in Fig. 8(b). It was also possible that, at the beginning, the lipid yield greatly depended on the excretion of amylolytic enzymes, but when the enzymes reached their minimum requirement the lipid yield was limited by other factors such as the amount of available carbon source or the carbon-to-nitrogen ratio.[68]

DISCUSSION

Aspergillus niger cell–CuS NBs

This study showed for the first time the enhanced production of the value-added products amylase, pyruvate and phenolic compounds by an *A. niger* cell–CuS NB system. The formation of NBs can be explained by the DLVO theory. Figure 3 shows changes in the structure of *A. niger* cell hyphae, and the EDX results reported in Fig. 4 confirm that most of the Cu and S was retained within the *A. niger* biomass, further confirming NB formation. The FTIR results (Fig. 5) confirm the presence of Cu—S bonds on the *A. niger* cells. To illustrate the photosensitizing behaviour of CuS NPs associated with *A. niger* cells, photoluminescence spectroscopy was used to confirm the electron transfer between CuS NPs and *A. niger* cells, as reported in Fig. 6. Cell membranes are semi-permeable and thus serve as barriers and gatekeepers for small-molecular-weight CuS NPs.[50,69] However, the passage of these molecules relies on specific transport proteins embedded in the membrane.[70]

The *A. niger* cell–CuS NB photosystem has both oxidative and reductive components and requires a sacrificial electron donor for the NP. Those components are the CuS NPs photocatalysts that harvest visible light and convert it into chemical potential, i.e. into reductive or oxidative potential that allows the sacrificial donor to provide electrons on the photoinduced CuS NP photocatalyst, thereby enhancing H^+ ions in the electron transport chain and the redox shuttling of electrons between CuS NPs and *A. niger* cells.[71,72] When the CuS NPs are present within the *A. niger* cells and exposed to a light source, the electrons move from the valence band to the conduction band (e^-), leaving positive holes (h^+). The electron transport chain stores these electrons; thus these electrons serve as a proton sink for the *A. niger* cells.[73] Figure 9 gives a pictorial representation of the *A. niger* cells–CuS NBs hybrid system. Organic electron shuttles, either produced by *A. niger* cells, i.e. flavins, phenazines and cysteine, or commonly found in the extracellular environment, i.e. media components, can facilitate electron transfer to the *A. niger* cells. Upon photoexcitation of CuS NPs, oxidation of cysteine (Cys) to cysteine (CySS) takes place and H^+ ions quench the valence band h^+, while the conduction band electron may be transferred to membrane-bound proteins.[74,75]

Proposed mechanism for value-added product formation by *A. niger* cell–CuS NBs

When *A. niger* cell–CuS NBs were exposed to light, the total lipid content increased with decrease in biomass dry weight, as shown in Fig. 8(a). Glycerophospholipids are by far the most abundant lipids in cell membranes, and lipids account for about half the mass of cell membranes.[51] Therefore, the total amino acid content remained constant in *A. niger* cell–CuS NBs, as shown in Fig. 8(a). In addition, lipid membranes are loaded with proteins. In fact, proteins account for roughly half the mass of most cellular membranes (Sperelakis, 2001).

The quantum efficiency was calculated, which is the ratio of incident photons converted into electrons, from photoluminescence data (Supporting Information, Table S1). The reducing equivalents present in the CuS NPs to *A. niger* cells NB entered mainly into the glycolysis pathway after acetyl-CoA synthesis via NADPH required for acetoacetyl-CoA reduction. For each mole of the value-added

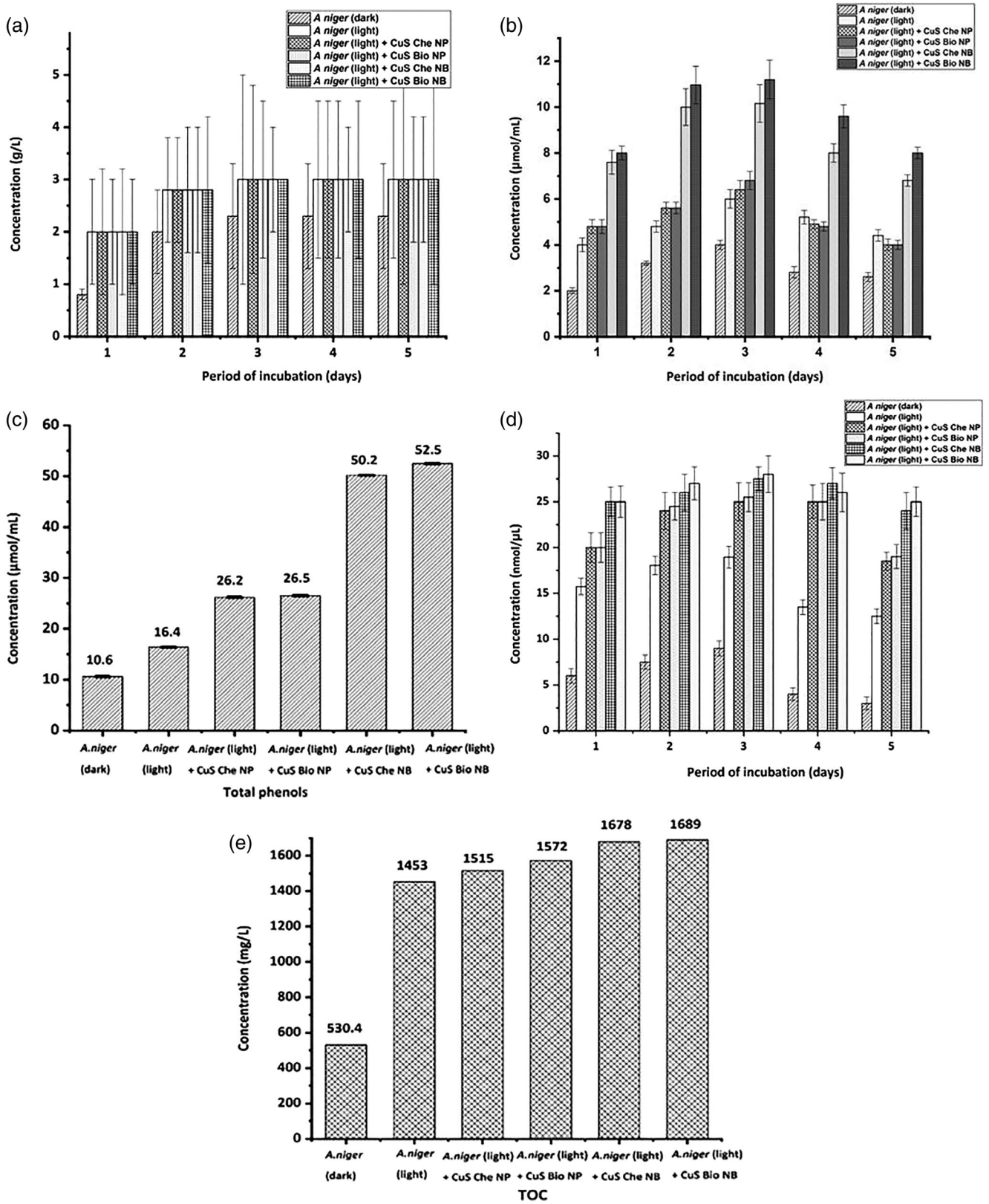

Figure 7. Concentration of (a) total sugars, (b) amylase activity, (c) total phenols, (d) pyruvate concentration and (e) TOC in various incubations of *A. niger*–CuS NBs and controls.

product (amylase, pyruvate and phenolic compounds) produced from acetoacetyl-CoA, 1 mol of $NADPH^+$ and H^+ is required, carrying 2 mol of electrons.[76–78]

The cellular respiration of NBs (glycolysis) generates ATP, and cells performing aerobic respiration synthesize much more ATP compared to *A. niger* cells.[79,80] These aerobic reactions use

Journal of Chemical Technology and Biotechnology published by John Wiley & Sons Ltd on behalf of Society of Chemical Industry (SCI).

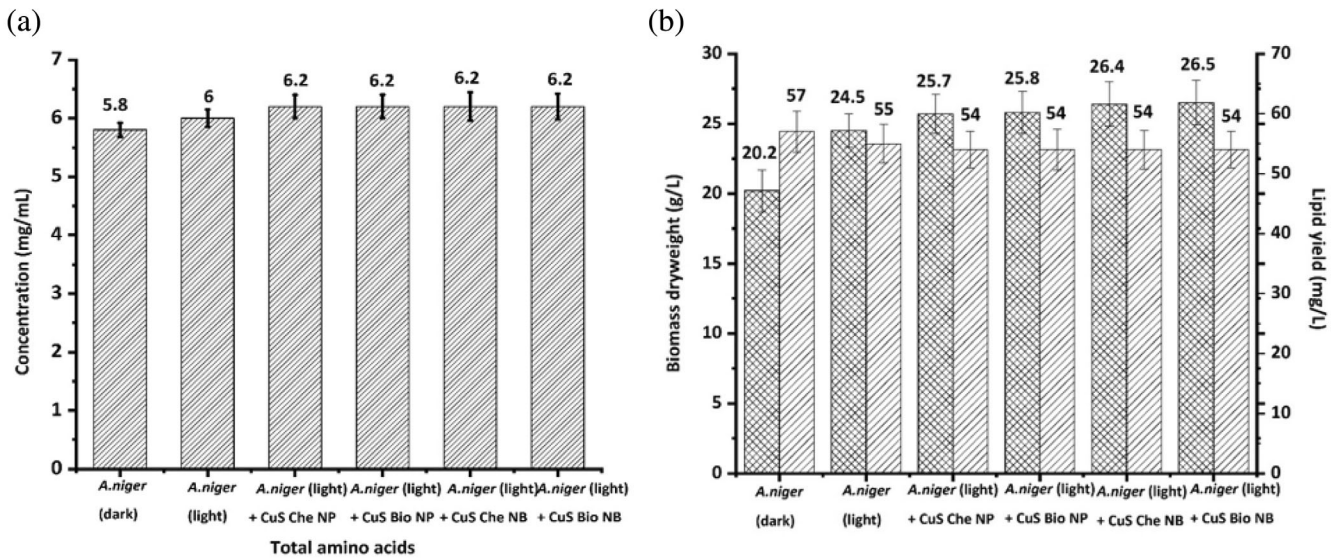

Figure 8. (a) Total amino acids and (b) lipid yield with respect to biomass dry weight of *A. niger* cells.

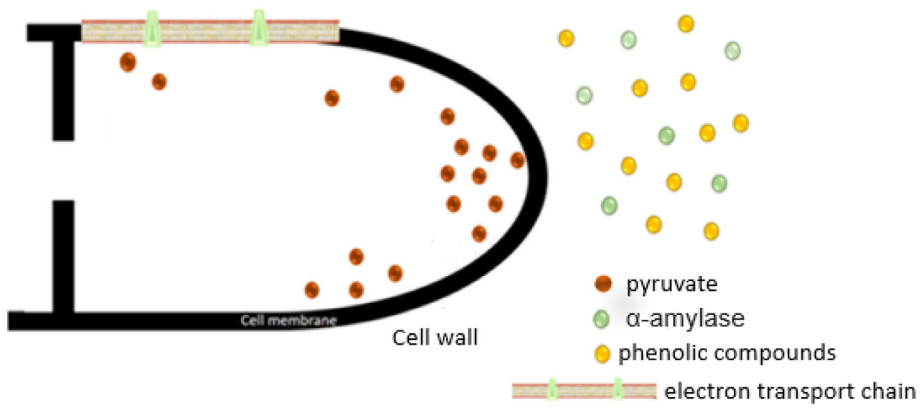

Figure 9. Schematic representation of formation of value-added products by *A. niger* cell–CuS NBs.

pyruvate, $NADH^+$ and H^+ from glycolysis. There is an increased availability of $NADH^+$ and H^+ in the *A. niger* cell–CuS NBs, thereby improving the amylase, pyruvate and phenolic compounds yield, as reported in Fig. 7(b)–(d). Therefore, the impact of light-driven *A. niger* cell–CuS NBs on intracellular NADPH/$NADP^+$ was significantly higher than that of *A. niger* cells grown in the absence of light. The CuS NBs produced the secondary metabolites amylase and phenolic compounds as well as the primary metabolite pyruvate. The secondary metabolites produced often depend on the environmental conditions and genetic make-up of the *A. niger* cells.[81,82] In *A. niger*, the shikimate pathway has been correlated with the production of phenolic compounds.

Sakimoto *et al.* (2016) highlighted the formation of *Moorella thermoacetica*–CdS bacterial cells. A similar study was conducted by Wang *et al.* (2019) to produce polyhydroxybutyrate using *Rhodopseudomonas palustris* with CdS NPs. However, studies on the production of value-added products are limited. Ding *et al.*[83] reported *Saccharomyces cerevisiae*–InP hybrids to produce shikimic acid, *Cupriavidus necator*–cadmium sulfide, cadmium selenide, indium phosphide, and copper zinc tin sulfide core–shell ZnS hybrids to produce methyl ketones, butanediol, ethylene, polyhydroxybutyrate and propanol. In our previous studies, we reported the use of *Aspergillus niger* cells–ZnS NB formation for enhanced degradation of methyl orange dye[32,33] and conducted experiments for the removal of benzene, toluene and xylene individually as well as in binary and trinary mixtures.[32,33]

However, in this study we have demonstrated the formation of CuS NPs embedded in the *A. niger* cells. The production yields of amylase, phenolic compounds and pyruvate were higher in *A. niger*–CuS NBs in comparison with solely *A. niger* cells and *A. niger* coincubated with CuS NPs. The *A. niger* coincubated with CuS Che NPs produced amylase (6.4 μmol mL^{-1}), pyruvate (25 nmol μL^{-1}) and phenols (26.2 μmol mL^{-1}); *A. niger* coincubated with CuS–Bio NPs produced 6.8 μmol mL^{-1} amylase, 25.5 nmol μL^{-1} pyruvate and 26.5 μmol mL^{-1} phenols. Conversely, *A. niger*–CuS NPs NBs were better in terms of production of amylase (11.2 μmol mL^{-1}), pyruvate (28 nmol μL^{-1}) and phenols (52.5 μmol mL^{-1}) for *A niger cells*–CuS–Bio NBs, and amylase (10.16 μmol mL^{-1}), pyruvate (27.5 nmol μL^{-1}) and phenols (50.2 μmol mL^{-1}) for *A niger* cells–CuS–Che NBs. This inorganic–bio hybrid system technology could become an alternative approach for the utilization of light energy to produce value-added chemicals in the near future.[91]

Practical implications

Industrial biotechnology has the potential to drive new growth, encourage innovation, boost productivity and address environmental/climatic issues.[84] In this regard, industrial biotechnology routes can replace many chemical production steps in terms of environmental and economic performance. At the same time, shifting from chemical to biological processes can result in a substantial reduction in carbon dioxide emissions and energy consumption, and allows the use of renewable substrates (Jenck *et al*., 2004; Hatti-Kaul *et al*., 2007).[85,86,88]

Using a traditional bioreactor with enzyme/chemical light-emitting diode panels, production using NBs may be simply scaled up from lab size to pilot scale, and potentially to commercial scale with configuration changes.[83] This can also be implemented by replacing light-emitting diode lamps with sunlight. Alternatively, other organisms, including those that directly absorb light such as algae or cyanobacteria,[87] can be used for NBs. Thus the NB platform has the potential for the direct and scalable production of renewable biofuels and bioproducts as well as a variety of enzymes from sunlight.[17]

CONCLUSIONS

In this study, CuS–Bio NPs showed higher amounts of amylase, pyruvate and phenolic compounds, i.e. 11.2 μmol mL^{-1}, 28 nmol μL^{-1} and 52.5 μmol mL^{-1}, respectively, for *A. niger*–CuS–Bio NBs in comparison to *A. niger*–CuS–Che NBs, as well as *A. niger*–CuS coincubated with Che NPs or Bio NPs. The *A. niger* cell–CuS NBs framework introduced here is a promising choice for use of light and chemical energy from NBs in a synergistic way to achieve higher yields than what can be accomplished with solely microbial-based processes. The CuS–Che spherical NPs exhibited a size range of 10–24 nm, whereas CuS–Bio spherical NPs had a typical size of 10–20 nm and nanorods a size of 100–150 nm, respectively. The band gap values (E_{bg}) were 1.3 eV and 1.6 eV for CuS–Che NPs and CuS–Bio NPs, respectively. The XRD patterns of both CuS Che NPs and CuS Bio NPs were in the hexagonal phase. The NB arrangement was affirmed by SEM by changes in the fungal hyphal structures and by the presence of peaks in the FTIR spectra. The presence of Cu and S in EDX affirmed the NB formation.

ACKNOWLEDGEMENTS

We thank our analytical team Borja Khatabi Soliman Tamayo, Leah Egan and Manuel Suarez at the National University of Ireland Galway (NUIG, Galway, Ireland) for help with the analysis. We would also like to thank Eadaoin Timmins and Emma McDermott from the Centre for Microscopy and Imaging (NUIG, Galway, Ireland) for providing TEM and SEM facilities. Further, we thank Patrick McArdle from the School of Chemistry (NUIG, Galway, Ireland) for providing the XRD facility. The authors acknowledge Science Foundation Ireland (SFI) for funding the Research Professorship *Innovative Energy Technologies for Biofuels, Bioenergy and a Sustainable Irish Bioeconomy* (IETSBIO3; Grant number 15/RP/2763) and the Research Infrastructure research grant *Platform for Biofuel Analysis* (Grant Number 16/RI/3401). Open access funding provided by IReL.

SUPPORTING INFORMATION

Supporting information may be found in the online version of this article.

REFERENCES

1 Raveendran S, Parameswaran B, Beevi Ummalyma S, Abraham A, Kuruvilla Mathew A, Madhavan A *et al*., Applications of microbial enzymes in food industry. *Food Technol Biotechnol* **56**:16–30 (2018). https://doi.org/10.17113/ftb.56.01.18.5491.
2 Panzella L, Moccia F, Nasti R, Marzorati S, Verotta L and Napolitano A, Bioactive phenolic compounds from agri-food wastes: An update on green and sustainable extraction methodologies. *Front Nutr* **7**: 60 (2020).
3 Tanyildizi MS, Özer D and Elibol M, Production of bacterial α-amylase by B. amyloliquefaciens under solid substrate fermentation. *Biochem Eng J* **37**:294–297 (2007).
4 Wang J, Li Y and Lu F, Molecular cloning and biochemical characterization of an α-amylase family from Aspergillus niger. *Electron J Biotechnol* **32**:55–62 (2018).
5 Suo H, Zhao X, Zhang Z, Wang Y, Sun J, Jin M *et al*., Rational design of ratiometric luminescence thermometry based on thermally coupled levels for bioapplications. *Laser Photonics Rev* **15**:2000319 (2021).
6 Xu Y, Bai H, Lu G, Li C and Shi G, Flexible graphene films via the filtration of water-soluble noncovalent functionalized graphene sheets. *J Am Chem Soc* **130**:5856–5857 (2008).
7 Taamalli A, Contreras MDM, Abu-Reidah IM, Trabelsi N and Ben Youssef N, Quality of phenolic compounds: Occurrence, health benefits, and applications in food industry. *J Food Qual* **2019** (2019).
8 Balasundram N, Sundram K and Samman S, Phenolic compounds in plants and agri-industrial by-products: Antioxidant activity, occurrence, and potential uses. *Food Chem* **99**:191–203 (2006).
9 Daoud FBO, Kaddour S and Sadoun T, Adsorption of cellulase *aspergillus Niger* on a commercial activated carbon: kinetics and equilibrium studies. *Colloids Surf, B* **75**:93–99 (2010). https://doi.org/10.1016/j.colsurfb.2009.08.019.
10 Yishai O, Lindner SN, de la Cruz JG, Tenenboim H and Bar-Even A, The formate bio-economy. *Curr Opin Chem Biol* **35**:1–9 (2016).
11 Carlsen M and Nielsen J, Influence of carbon source on α-amylase production by *aspergillus oryzae*. *Appl Microbiol Biotechnol* **57**:346–349 (2001). https://doi.org/10.1007/s002530100772.
12 Riyaz S, Parveen A and Azam A, Microstructural and optical properties of CuS nanoparticles prepared by sol–gel route. *Perspect Sci* **8**:632–635 (2016). https://doi.org/10.1016/j.pisc.2016.06.041.
13 Dutta A and Dolui SK, Preparation of colloidal dispersion of CuS nanoparticles stabilized by SDS. *Mater Chem Phys* **112**:448–452 (2008). https://doi.org/10.1016/j.matchemphys.2008.05.072.
14 Mageshwari K, Mali SS, Hemalatha T, Sathyamoorthy R and Patil PS, Low temperature growth of CuS nanoparticles by reflux condensation method. *Prog Solid State Chem* **39**:108–113 (2011). https://doi.org/10.1016/j.progsolidstchem.2011.10.003.
15 Nemade KR and Waghuley SA, Band gap engineering of CuS nanoparticles for artificial photosynthesis. *Mater Sci Semicond Process* **39**: 781–785 (2015). https://doi.org/10.1016/j.mssp.2015.05.045.
16 Sakimoto KK, Liu C, Lim J and Yang P, Salt-induced self-assembly of bacteria on nanowire arrays. *Nano Lett* **14**:5471–5476 (2014). https://doi.org/10.1021/nl502946j.
17 Zhang H, Liu H, Tian Z, Lu D, Yu Y, Cestellos-Blanco S *et al*., Bacteria photosensitized by intracellular gold nanoclusters for solar fuel production. *Nat Nanotechnol* **13**:900–905 (2018). https://doi.org/10.1038/s41565-018-0267-z.
18 Negi BB, Sinharoy A and Pakshirajan K, Selenite removal from wastewater using fungal pelleted airlift bioreactor. *Environ Sci Pollut Res* **27**:992–1003 (2020).
19 Fajardo-Cavazos P, Leehan JD and Nicholson WL, Alterations in the spectrum of spontaneous rifampicin-resistance mutations in the Bacillus subtilis rpoB gene after cultivation in the human spaceflight environment. *Front Microbiol* **9**:192 (2018).
20 Dash BK, Rahman MM and Sarker PK, Molecular identification of a newly isolated *Bacillus subtilis* BI19 and optimization of production conditions for enhanced production of extracellular amylase. *Biomed Res Int* **2015**:1–9 (2015). https://doi.org/10.1155/2015/859805.
21 Gigras P, Sahai V and Gupta R, Statistical media optimization and production of ITS α-amylase from *aspergillus oryzae* in a bioreactor. *Curr Microbiol* **45**:203–208 (2002). https://doi.org/10.1007/s00284-001-0107-4.
22 Mu C and He J, Confined conversion of CuS nanowires to CuO nanotubes by annealing-induced diffusion in nanochannels. *Nanoscale Res Lett* **6**:150 (2011). https://doi.org/10.1186/1556-276X-6-150.

Journal of Chemical Technology and Biotechnology published by John Wiley & Sons Ltd on behalf of Society of Chemical Industry (SCI).

23 Sutradhar P and Saha M, Green synthesis of zinc oxide nanoparticles using tomato (*Lycopersicon esculentum*) extract and its photovoltaic application. *J Exp Nanosci* **11**:314–327 (2016). https://doi.org/10.1080/17458080.2015.1059504.
24 Castilla-Archilla J, Papirio S and Lens PN, Two step process for volatile fatty acid production from brewery spent grain: hydrolysis and direct acidogenic fermentation using anaerobic granular sludge. *Process Biochem* **100**:272–283 (2021).
25 Tan LC, Lin R, Murphy JD and Lens PN, Granular activated carbon supplementation enhances anaerobic digestion of lipid-rich wastewaters. *Renewable Energy* **171**:958–970 (2021).
26 Abinaya M, Vaseeharan B, Divya M, Sharmili A, Govindarajan M, Alharbi NS *et al*., Bacterial exopolysaccharide (EPS)-coated ZnO nanoparticles showed high antibiofilm activity and larvicidal toxicity against malaria and Zika virus vectors. *J Trace Elem Med Biol* **45**: 93–103 (2018). https://doi.org/10.1016/j.jtemb.2017.10.002.
27 Chawla P, Najda A, Bains A, Nurzyńska-Wierdak R, Kaushik R and Tosif MM, Potential of gum arabic functionalized iron hydroxide nanoparticles embedded cellulose paper for packaging of paneer. *Nanomaterials* **11**:1–14 (2021). https://doi.org/10.3390/nano11051308.
28 Derjaguin BV, Churaev NV, Muller VM and Kisin VI, *Surface Forces*. Consultants Bureau, New York (1987).
29 Ohshima H, Approximate analytic expression for the stability ratio of colloidal dispersions. *Colloid Polym Sci* **292**:2269–2274 (2014).
30 Liu C, Gallagher JJ, Sakimoto KK, Nichols EM, Chang CJ, Chang MCY *et al*., Nanowire-bacteria hybrids for unassisted solar carbon dioxide fixation to value-added chemicals. *Nano Lett* **15**:3634–3639 (2015). https://doi.org/10.1021/acs.nanolett.5b01254.
31 Chen KL and Elimelech M, Influence of humic acid on the aggregation kinetics of fullerene (C60) nanoparticles in monovalent and divalent electrolyte solutions. *J Colloid Interface Sci* **309**:126–134 (2007).
32 Uddandarao P and Lens PN, Light driven *aspergillus Niger*-ZnS nanobiohybrids for degradation of methyl orange. *Chemosphere* **298**:134–162 (2022a). https://doi.org/10.1016/j.chemosphere.2022.134162.
33 Uddandarao P and Lens PN, Enhanced removal of hydrocarbons BTX by light-driven *aspergillus Niger* ZnS nanobiohybrids. *Enzyme Microb Technol* **157**:110020 (2022b). https://doi.org/10.1016/j.enzmictec.2022.110020.
34 Mabel SH, Rodríguez MR, Guerra NP and Rosés RP, Amylase production by Aspergillus niger in submerged cultivation on two wastes from food industries. *J Food Eng* **73**:93–100 (2006).
35 Gomes TA, Zanette CM and Spier MR, An overview of cell disruption methods for intracellular biomolecules recovery. *Prep Biochem Biotechnol* **7**:635–654 (2020).
36 Ho CW, Chew TK, Ling TC, Kamaruddin S, Tan WS and Tey BT, Efficient mechanical cell disruption of *Escherichia coli* by an ultrasonicator and recovery of intracellular hepatitis B core antigen. *Process Biochem* **41**:1829–1834 (2006). https://doi.org/10.1016/j.procbio.2006.03.043.
37 Liu D, Zeng XA, Sun DW and Han Z, Disruption and protein release by ultrasonication of yeast cells. *Innov Food Sci Emerg Technol* **18**: 132–137 (2013). https://doi.org/10.1016/j.ifset.2013.02.006.
38 Debebe A, Temesgen S, Redi-Abshiro M, Chandravanshi BS and Ele E, Improvement in analytical methods for determination of sugars in fermented alcoholic beverages. *J Anal Methods Chem* **2018**:1–10 (2018). https://doi.org/10.1155/2018/4010298.
39 Nielsen SS, Phenol-sulfuric acid method for total carbohydrates, in *Food Analysis Laboratory Manual*. Springer, Boston, MA, pp. 47–53 (2010).
40 Breuil C and Saddler JN, Comparison of the 3,5-dinitrosalicylic acid and Nelson-Somogyi methods of assaying for reducing sugars and determining cellulase activity. *Enzyme Microb Technol* **7**:327–332 (1985).
41 Hasan MM, Marzan LW, Hosna A, Hakim A and Azad AK, Optimization of some fermentation conditions for the production of extracellular amylases by using *Chryseobacterium* and *bacillus* isolates from organic kitchen wastes. *J Genet Eng Biotechnol* **15**:59–68 (2017). https://doi.org/10.1016/j.jgeb.2017.02.009.
42 Naili B, Sahnoun M, Bejar S and Kammoun R, Optimization of submerged *aspergillus oryzae* S2 α-amylase production. *Food Sci Biotechnol* **25**: 185–192 (2016). https://doi.org/10.1007/s10068-016-0028-4.
43 Sahnoun M, Kriaa M, Elgharbi F, Ayadi DZ, Bejar S and Kammoun R, *Aspergillus oryzae* S2 alpha-amylase production under solid state fermentation: optimization of culture conditions. *Int J Biol Macromol* **75**:73–80 (2015). https://doi.org/10.1016/j.ijbiomac.2015.01.026.
44 Berges JA, Fisher AE and Harrison PJ, A comparison of Lowry, Bradford and smith protein assays using different protein standards and protein isolated from the marine diatom *Thalassiosira pseudonana*. *Mar Biol* **115**:187–193 (1993).
45 Mukherjee R, Paul T, Soren JP, Halder SK, Mondal KC, Pati BR *et al*., Acidophilic α-amylase production from *aspergillus Niger* RBP7 using potato peel as substrate: a waste to value added approach. *Waste Biomass Valorization* **10**:851–863 (2019). https://doi.org/10.1007/s12649-017-0114-8.
46 Arora DS and Chandra P, Antioxidant activity of *aspergillus fumigatus*. *ISRN Pharmacol* **2011**:1–11 (2011). https://doi.org/10.5402/2011/619395.
47 Blainski A, Lopes GC and De Mello JCP, Application and analysis of the folin ciocalteu method for the determination of the total phenolic content from *Limonium brasiliense* L. *Molecules* **18**:6852–6865 (2013). https://doi.org/10.3390/molecules18066852.
48 Noreen H, Semmar N, Farman M and McCullagh JSO, Measurement of total phenolic content and antioxidant activity of aerial parts of medicinal plant *Coronopus didymus*. *Asian Pac J Trop Med* **10**:792–801 (2017). https://doi.org/10.1016/j.apjtm.2017.07.024.
49 Zhang H, Duan S, Radjenovic PM, Tian ZQ and Li JF, Core–shell nanostructure-enhanced Raman spectroscopy for surface catalysis. *Acc Chem Res* **53**:729–739 (2020).
50 Gautier A and Hinner MJ, *Site-Specific Protein Labeling*. Springer, New York (2015).
51 Coskun Ü and Simons K, Cell membranes: the lipid perspective. *Structure* **19**:1543–1548 (2011).
52 Dipankar C and Murugan S, The green synthesis, characterization and evaluation of the biological activities of silver nanoparticles synthesized from Iresine herbstii leaf aqueous extracts. *Colloids Surf, B* **98**: 112–119 (2012).
53 Nethravathi C, Nath R, Rajamathi JT and Rajamathi M, Microwave-assisted synthesis of porous aggregates of CuS nanoparticles for sunlight photocatalysis. *ACS Omega* **4**:4825–4831 (2019). https://doi.org/10.1021/acsomega.8b03288.
54 Kalanur SS and Seo H, Tuning plasmonic properties of CuS thin films via valence band filling. *RSC Adv* **7**:11118–11122 (2017). https://doi.org/10.1039/c6ra27076j.
55 Sun W, Meng S, Zhang S, Zheng X, Ye X, Fu X *et al*., Insight into the transfer mechanisms of photogenerated carriers for heterojunction photocatalysts with the analogous positions of valence band and conduction band: a case study of ZnO/TiO_2. *J Phys Chem C* **122**: 15409–15420 (2018). https://doi.org/10.1021/acs.jpcc.8b03753.
56 Tan HL, Abdi FF and Ng YH, Heterogeneous photocatalysts: an overview of classic and modern approaches for optical, electronic, and charge dynamics evaluation. *Chem Soc Rev* **48**:1255–1271 (2019). https://doi.org/10.1039/c8cs00882e.
57 Zhou X, Wierzbicka E, Liu N and Schmuki P, Black and white anatase, rutile and mixed forms: band-edges and photocatalytic activity. *Chem Commun* **55**:533–536 (2019). https://doi.org/10.1039/c8cc07665k.
58 Chen J, Wu L, Lu M, Lu S, Li Z and Ding W, Comparative study on the fungicidal activity of metallic MgO nanoparticles and macroscale MgO against soilborne fungal phytopathogens. *Front Microbiol* **11**: 1–19 (2020). https://doi.org/10.3389/fmicb.2020.00365.
59 Rosário J, da Luz LL, Geris R, Ramalho JGS, da Silva AF, Júnior SA *et al*., Photoluminescent organisms: how to make fungi glow through biointegration with lanthanide metal-organic frameworks. *Sci Rep* **9**:1–10 (2019). https://doi.org/10.1038/s41598-019-43835-x.
60 Bhat R, Potential use of fourier transform infrared spectroscopy for identification of molds capable of producing mycotoxins. *Int J Food Prop* **16**:1819–1829 (2013). https://doi.org/10.1080/10942912.2011.609629.
61 Gáplovská K, Šimonovičová A, Halko R, Okenicová L, Žemberyová M, Čerňanský S *et al*., Study of the binding sites in the biomass of aspergillus Niger wild-type strains by FTIR spectroscopy. *Chem Pap* **72**: 2283–2288 (2018). https://doi.org/10.1007/s11696-018-0487-6.
62 Saranya M, Santhosh C, Ramachandran R and Nirmala Grace A, Growth of CuS nanostructures by hydrothermal route and its optical properties. *J Nanotechnol* **321571**:1–8 (2014). https://doi.org/10.1155/2014/321571.
63 Wang Y, Jiang F, Chen J, Sun X, Xian T and Yang H, In situ construction of CNT/CuS hybrids and their application in photodegradation for

Journal of Chemical Technology and Biotechnology published by John Wiley & Sons Ltd on behalf of Society of Chemical Industry (SCI).

removing organic dyes. *Nanomaterials* **10**:1–19 (2020). https://doi.org/10.3390/nano10010178.
64 Kumaran S, Abdelhamid HN and Wu HF, Quantification analysis of protein and mycelium contents upon inhibition of melanin for: *aspergillus Niger*: a study of matrix assisted laser desorption/ ionization mass spectrometry (MALDI-MS). *RSC Adv* **7**:30289–30294 (2017). https://doi.org/10.1039/c7ra03741d.
65 Redmile-Gordon MA, Armenise E, White RP, Hirsch PR and Goulding KWT, A comparison of two colorimetric assays, based upon Lowry and Bradford techniques, to estimate total protein in soil extracts. *Soil Biol Biochem* **67**:166–173 (2013). https://doi.org/10.1016/j.soilbio.2013.08.017.
66 Cheirsilp B and Kitcha S, Solid state fermentation by cellulolytic oleaginous fungi for direct conversion of lignocellulosic biomass into lipids: fed-batch and repeated-batch fermentations. *Ind Crops Prod* **66**:73–80 (2015). https://doi.org/10.1016/j.indcrop.2014.12.035.
67 Converti A, Casazza AA, Ortiz EY, Perego P and Del Borghi M, Effect of temperature and nitrogen concentration on the growth and lipid content of *Nannochloropsis oculata* and *Chlorella vulgaris* for biodiesel production. *Chem Eng Process: Process Intensif* **48**:1146–1151 (2009). https://doi.org/10.1016/j.cep.2009.03.006.
68 Miranda AF, Taha M, Wrede D, Morrison P, Ball AS, Stevenson T *et al*., Lipid production in association of filamentous fungi with genetically modified cyanobacterial cells. *Biotechnol Biofuels* **8**:1–18 (2015). https://doi.org/10.1186/s13068-015-0364-2.
69 Trimble WS and Grinstein S, Barriers to the free diffusion of proteins and lipids in the plasma membrane. *J Cell Biol* **208**:259–271 (2015). https://doi.org/10.1083/jcb.201410071.
70 Cooper GM, Transport of small molecules, in *The Cell: A Molecular Approach*, 2nd edn. Sinauer Associates, Sunderland (MA) (2000).
71 Graml A, Neveselý T, Jan Kutta R, Cibulka R and König B, Deazaflavin reductive photocatalysis involves excited semiquinone radicals. *Nat Commun* **11**:1–11 (2020). https://doi.org/10.1038/s41467-020-16909-y.
72 Yamazaki Y, Takeda H and Ishitani O, Photocatalytic reduction of CO_2 using metal complexes. *J Photochem Photobiol C* **25**:106–137 (2015).
73 Han Z, Zheng X, Hu F, Qu F, Umar A and Wu X, Facile synthesis of hollow ZnS nanospheres for environmental remediation. *Mater Lett* **160**:271–274 (2015). https://doi.org/10.1016/j.matlet.2015.07.152.
74 Martín SS, Rivero MJ and Ortiz I, Unravelling the mechanisms that drive the performance of photocatalytic hydrogen production. *Catalysts* **10**:1–27 (2020). https://doi.org/10.3390/catal10080901.
75 Narayanam JMR and Stephenson CRJ, Visible light photoredox catalysis: applications in organic synthesis. *Chem Soc Rev* **40**:102–113 (2011). https://doi.org/10.1039/b913880n.
76 Kocharin K, Chen Y, Siewers V and Nielsen J, Engineering of acetyl-CoA metabolism for the improved production of polyhydroxybutyrate in *Saccharomyces cerevisiae*. *AMB Express* **2**:1–11 (2012). https://doi.org/10.1186/2191-0855-2-52.
77 Kocharin K, Siewers V and Nielsen J, Improved polyhydroxybutyrate production by Saccharomyces cerevisiae through the use of the phosphoketolase pathway. *Biotechnol Bioeng* **110**:2216–2224 (2013). https://doi.org/10.1002/bit.24888.
78 Satowa D, Fujiwara R, Uchio S, Nakano M, Otomo C, Hirata Y *et al*., Metabolic engineering of *E. coli* for improving mevalonate production to promote NADPH regeneration and enhance acetyl-CoA supply. *Biotechnol Bioeng* **117**:2153–2164 (2020). https://doi.org/10.1002/bit.27350.
79 Bujara M, Schümperli M, Pellaux R, Heinemann M and Panke S, Optimization of a blueprint for in vitro glycolysis by metabolic real-time analysis. *Nat Chem Biol* **7**:271–277 (2011).
80 Zaytseva YY, Harris JW, Mitov MI, Kim JT, Butterfield DA, Lee EY *et al*., Increased expression of fatty acid synthase provides a survival advantage to colorectal cancer cells via upregulation of cellular respiration. *Oncotarget* **22**:18891–18904 (2015).
81 Calvo AM, Wilson RA, Bok JW and Keller NP, Relationship between secondary metabolism and fungal development. *Microbiol Mol Biol Rev* **66**:447–459 (2002).
82 Tavares DG, Barbosa BVL, Ferreira RL, Duarte WF and Cardoso PG, Antioxidant activity and phenolic compounds of the extract from pigment-producing fungi isolated from Brazilian caves. *Biocatal Agric Biotechnol* **16**:148–154 (2018).
83 Ding Y, Bertram JR, Eckert C, Bommareddy RR, Patel R, Conradie A *et al*., Nanorg microbial factories: light-driven renewable biochemical synthesis using quantum dot-bacteria nanobiohybrids. *J Am Chem Soc* **141**:10272–10282 (2019). https://doi.org/10.1021/jacs.9b02549.
84 Gao S and Zhang H, Urban planning for low-carbon sustainable development. *Sustainable Comput: Inf Syst* **28**:100398 (2020).
85 Jenck JF, Agterberg F and Droescher MJ, Products and processes for a sustainable chemical industry: a review of achievements and prospects. *Green Chem* **6**:544–556 (2004).
86 Hatti-Kaul R, Törnvall U, Gustafsson L and Börjesson P, Industrial biotechnology for the production of bio-based chemicals–a cradle-to-grave perspective. *Trends Biotechnol* **25**:119–124 (2007).
87 Liu Z, Wang K, Chen Y, Tan T and Nielsen J, Third-generation biorefineries as the means to produce fuels and chemicals from CO2. *Nat Catal* **3**:274–288 (2020).
88 Cherubini F, The biorefinery concept: using biomass instead of oil for producing energy and chemicals. *Energ Conver Manage* **51**:1412–1421 (2010).
89 Kornienko N, Sakimoto KK, Herlihy DM, Nguyen SC, Alivisatos AP, Harris CB *et al*., Spectroscopic elucidation of energy transfer in hybrid inorganic-biological organisms for solar-to-chemical production. *Proc Natl Acad Sci* **113**:11750–11755 (2016). https://doi.org/10.1073/pnas.1610554113.
90 Kuriakose S, Hitha H, Jose A, John M and Varghese T, Structural and optical characterization of lanthanum tungstate nanoparticles synthesized by chemical precipitation route and their photocatalytic activity. *Opt Mater* **99**:109571 (2020).
91 Liu C, Sakimoto KK, Colón BC, Silver PA and Nocera DG, Ambient nitrogen reduction cycle using a hybrid inorganic–biological system. *Proc Natl Acad Sci* **114**:6450–6455 (2017).
92 Hernandez PA, Graham CH, Master LL and Albert DL, The effect of sample size and species characteristics on performance of different species distribution modeling methods. *Ecography* **29**:773–785 (2006).
93 Folch J, Lees M and Sloane Stanley GH, A simple method for the isolation and purification of total lipids from animal tissues. *J Biol Chem* **226**:497–509 (1957).
94 Vijayakumar M, Priya K, Nancy FT, Noorlidah A and Ahmed ABA, Biosynthesis, characterisation and anti-bacterial effect of plant-mediated silver nanoparticles using Artemisia nilagirica. *Ind Crops Prod* **41**:235–240 (2013).
95 Amirian F, Molaei M, Karimipour M and Bahador AR, A new and simple UV-assisted approach for synthesis of water soluble ZnS and transition metals doped ZnS nanoparticles (NPs) and investigating optical and photocatalyst properties. *J Lumin* **196**:174–180 (2018).
96 Sánchez-Rodríguez E, Moreno DA, Ferreres F, del Mar Rubio-Wilhelmi M and Ruiz JM, Differential responses of five cherry tomato varieties to water stress: changes on phenolic metabolites and related enzymes. *Phytochemistry* **72**:723–729 (2011).

